



Mechanistic roles of catalyst surface coating in nitrobenzene selective reduction: A first-principles study



Li Gong^{a,b}, Yang Mu^{a,*}, Michael J. Janik^{b,*}

^a Department of Chemistry, University of Science and Technology of China, Hefei, China

^b Department of Chemical Engineering, The Pennsylvania State University, University Park, PA 16802, USA

ARTICLE INFO

Keywords:

Nitrobenzene
Phenylhydroxylamine
DFT
Organic modifiers
Selective reduction

ABSTRACT

Adsorbed organic modifiers can alter selectivity of metal catalysts by modifying reactant, intermediate, or product adsorption affinities and configurations. Herein, we show how alkylamine self-assembled monolayers with varying surface densities can be used to tune selectivity to desired hydrogenation products of nitrobenzene (NB) reduction on a Pt (111) catalyst. Nitrobenzene is a toxic environmental pollutant with deleterious health effects, and its selective conversion to valuable chemicals can both convert this pollutant and improve catalytic process efficiency. Density functional theory (DFT) calculations demonstrate that the selectivity of NB reduction to phenylhydroxylamine (PHA) is achieved by controlling the surface crowding, with specific sites exposed for the selective reduction of NB on the Pt (111) surface through the selection of alkylamine modifier surface density. Surface crowding forces NB and subsequent reaction intermediates to bind with their long axis vertical to the Pt (111) surface, increasing the selectivity to the desired product, PHA. This surface crowding serves both to enhance selectivity and provide insight into the reaction mechanism of NB reduction.

1. Introduction

In homogeneous catalysis and biocatalysis, ligands on catalytically active metal centers often induce significant steric and electronic effects that impact the overall selectivity and catalytic activity. Organic modifiers (ligands) on metal-based heterogeneous catalysts have been used to similarly enhance either the catalytic activity or selectivity [1–3]. Ligands can affect the electronic characteristics of surface sites or induce steric effects to change the substrate molecules access to the catalyst surface [2]. For example, self-assembled monolayer coatings of n-alkane thiols enhanced the selectivity of furfural/furfural alcohol hydrodeoxygenation on Pd nano-catalysts through blocking non-selective sites and promoting a specific adsorbate orientation [4,5]. Alkylamine-capped Pt₃Co nanocatalysts improved hydrogenation selectivity of α, β-unsaturated aldehydes to α, β-unsaturated alcohols through steric effects that limited over-hydrogenation [6]. The use of organic modifiers to control selectivity in nitrobenzene (NB) reduction was demonstrated by Chen et al. [7] Chen et al. synthesized ethylenediamine-coated ultrathin platinum nanowires that increased selectivity of NB reduction to phenylhydroxylamine (PHA). The authors attributed the increased selectivity to an interfacial electronic effect, [7] though the evidence for the mechanistic cause of the increased selectivity was limited. Determination of the mechanistic source of organic modifier

effects on selective reduction can provide guidance in further optimizing heterogeneous catalysts for the selective reduction of NB to PHA.

Nitrobenzene has been widely recognized as a toxic environmental pollutant and poses great threat to human health [8,9]. Catalytic hydrogenation of nitrobenzene is not only a reaction of environmental importance, but also is industrially relevant for producing aniline (AN), hydroxylamine and azobenzene products [10–12]. Achieving high product selectivity is essential to advancing this process. Selective catalytic reduction of nitrobenzene to PHA could find significant application, as PHA is a valuable synthetic platform species with numerous commodity outlets [13]. PHA can undergo rearrangement to yield a variety of substituted anilines such as p-aminophenol, p-anisidine, p-phenitidine, and p-chloroaniline in acid conditions. Under alkaline conditions, PHA can react with nitrosobenzene (NSB) to form azoxybenzene and azobenzene, which have applications as organic dyes, food additives and therapeutic agents. Organic hydroxylamines are also useful as intermediates in the synthesis of biologically active substances, reagents for organic synthesis, and raw materials for a polymerization inhibitor [14–17]. However, little attention has been devoted to selective reduction of nitrobenzene to PHA, compared with reduction to AN.

PHA can be formed by hydrogenation of NB using supported noble

* Corresponding authors.

E-mail addresses: yangmu@ustc.edu.cn (Y. Mu), mjanik@engr.psu.edu (M.J. Janik).

metal catalysts, catalysts in organic solvent, and metal catalysts with promoters [13,18–20]. As NB has multiple functional groups, the selectivity towards the desired product (PHA) is a significant challenge in heterogeneous catalysis. PHA is commonly synthesized by 1) zinc-catalyzed reduction of NB in the aqueous phase in the presence of NH₄Cl as a promoter or 2) rhodium-catalyzed hydrogenation of nitrobenzene, using hydrazine as an H₂ source, with AN as the major byproduct [21–26]. Studies have been focused on using different promoters to enhance the selectivity of PHA/AN, for example, NaCl and NH₄Cl for Zn catalysts, or Me₂SO for Pt catalysts [13,27]. However, these promoters can also poison catalysts or corrode the reactor. Selective heterogeneous catalytic hydrogenation of NB is an ideal process to produce PHA as this process could be environmentally and economically benign [20,27]. Highly selective catalysts are still needed to arrest reduction at PHA versus completely hydrogenating the N moiety to AN.

We apply density functional theory (DFT) calculations to investigate the mechanistic explanation for selective reduction of NB to PHA tuned by organic surface modification. We systematically explored structures of alkylamines of different chain length with various packing density on Pt (111) surfaces and their impact on the NB reduction elementary reaction sequence. Alkylamine coated on the Pt (111) surface alters the preferred adsorption configuration of NB reduction intermediates and the energetics of NB reduction elementary steps, relative to the bare Pt (111) surface. The PHA desorption energy and the energy barriers for PHA hydrogenation were calculated to explore the selectivity of NB reduction to PHA. NB reduction on Pt-based alloy surfaces were further explored to consider whether the addition of an inert metal could provide similar alterations in elementary energetics as amine modifiers.

2. Methods

DFT calculations were performed within the Vienna Ab initio simulation package (VASP, version 5.3.5), using the periodic supercell approach. The projector augmented wave (PAW) method was used for electron-ion interactions. The Perdew-Burke-Ernzerhof functional with a dispersion correction (PBE-D3) described the electron-electron exchange and correlation energies [28,29]. PBE-D3 was previously used to examine the impact of self-assembled monolayers on Pd and Cu surfaces and provided mechanistic behavior consistent with experiment [4,30]. A plane wave basis set was used with an energy cutoff of 400 eV. For geometry optimization, the convergence criteria of the forces acting on atoms was 0.05 eV/Å, while the energy threshold-defining self-consistency of the electron density was 10⁻⁵ eV. Transition state structure searches used the climbing image nudged elastic band (CI - NEB) method [31].

3. Model and calculations

The Pt (111) metal slab is composed of five atomic layers, with the bottom three layers frozen at their bulk positions during structural optimization. The vacuum between the bare Pt (111) slabs before adding reaction intermediates is 20 Å to avoid interactions between periodic slabs. For the 1/9, 1/6, 1/4 and 1/3 monolayer (ML) alkylamine capped Pt (111) surfaces, 3 × 3, 2 × 3, 2 × 2 and r3 × r3 unit cells were used respectively. For models considering amine adsorption, the vacuum region was increased to 30 Å to avoid interactions between periodic slabs. The surface structural relaxation and the total energy calculation of 3 × 3, 2 × 3, 2 × 2 and r3 × r3 supercell units were performed with 5 × 5 × 1, 7 × 7 × 1, 9 × 9 × 1 and 9 × 9 × 1 Monkhorst – Pack [32] mesh k-space sampling grids, respectively [33]. The geometries of all surface NB reduction intermediates were fully optimized.

The adsorption energies of surface species (ΔE_{ads}) were calculated using Eq. (1):

$$\Delta E_{ads} = E_{species+surface} - E_{species} - E_{surface} \quad (1)$$

where $E_{species}$ is the energy of the isolated intermediate, $E_{surface}$ is the energy of the bare surface (or amine adsorbed surface for considering adsorption in the presence of the amine), and $E_{species+surface}$ is the energy of the intermediate adsorbed on the surface. A negative ΔE_{ads} corresponds to a stable adsorbate–surface system.

All relative energies presented are zero point vibrational energy (ZPVE) corrected and include a vibrational entropy term. The free energy of an adsorbed intermediate ($G_{species}^*$) is calculated as:

$$G_{species}^* = E_{species}^* + E_{ZPVE} + E_{vib} - TS_{vib} \quad (2)$$

where $E_{species}^*$ is the DFT optimized energy of the adsorbed intermediate, E_{ZPVE} is the zero-point vibrational energy, E_{vib} is the internal energy stored in vibration at 300 K, and TS_{vib} represents the vibrational entropy of the adsorbed species at room temperature (300 K). Harmonic vibrational modes were calculated only for the adsorbate atoms.

Reaction energetics for NB reduction are determined by calculating free energy differences among surface intermediates, with any H species involved in the reaction considered relative to a gas-phase hydrogen molecule. The gas phase free energy of the H₂ molecular species was calculated using a large unit cell and including both a zero point vibrational energy (ZPVE) correction, translational and rotational entropy as well as a vibrational entropy term.

4. Results and discussion

4.1. Adsorption of alkylamines on the Pt (111) surface

Experimental and theoretical studies of alkylamine-capped Pt nanoparticles have come to the conclusion that the N atom of NH₂ bonds to the Pt (111) surface and the alkyl tails are oriented away from the surface [6,34]. We first considered various possible locations of the ethylamine (C₂-NH₂) N atom with respect to the Pt (111) high symmetry sites: atop (t), bridge (b), 3-fold hollow site (both face centered cubic (fcc) and hexagonal close packed (hcp) sites)). We then probed the geometries and energies of alkylamine adsorption on the Pt (111) surfaces at different capping coverages of 1/9, 1/6, 1/4 and 1/3 ML.

As shown in Table 1, the binding energies of C₂-NH₂ at 1/9, 1/6, 1/3 and 1/2 ML Pt (111) surfaces ranged from −1.0 to −1.8 eV, slightly weaker than for hexadecylamine adsorption on the Cu (111) surface. [30] Weaker binding may be due to the short chain length of C₂-NH₂, as binding of alkane thiols was shown to increase on Pd surfaces with increasing chain length [4]. C₂-NH₂ preferred to reside with the N atom above the atop site, regardless of amine coverage. This is consistent with prior DFT calculations of hexadecylamine on the atop sites of the Cu (111) surface [30] and experimental indication that methylamines preferred atop sites of Au (111) [35].

As shown in Table 2, for all capping coverages above 1/9 ML, the energies of alkylamine on the Pt (111) surfaces strengthened with increasing alkyl chain length due to the higher van der Waals (vdW) attraction among the longer alkyl tails. Alkylamine binding energies as a function of alkyl chain length on the Pt (111) surfaces, with coating densities of 1/9, 1/6, 1/4, 1/3 ML, are summarized in Fig. S1. Optimized structures of C₆-NH₂ on the 1/3, 1/4, 1/6 and 1/9 ML Pt (111) surfaces are illustrated in Fig. 1. At the 1/9 ML coverage, the binding strength of alkylamines fluctuated slightly with the alkyl chain length

Table 1

The adsorption energy of C₂-NH₂ on Pt (111) surfaces at different coverage. Unit: eV.

	1/3 ML	1/4 ML	1/6 ML	1/9 ML
atop	−1.21	−1.37	−1.48	−1.64
brg	−1.17	−1.25	−1.41	−1.58
hcp	−1.17	−1.20	−1.29	−1.50
fcc	−1.07	−1.12	−1.43	−1.60

Table 2

The optimized properties of different chain length alkylamine on the Pt (111) surface at different coverage: 1/9, 1/6, 1/4 and 1/3 ML: tilt angle ($^\circ$), adsorption energy (E_{ads}), dispersion energy (E_{disp}).

Chain length	1/3 ML			1/4 ML			1/6 ML			1/9 ML	
	Angle ($^\circ$)	E_{ads} (eV)	E_{disp} (eV)	Angle ($^\circ$)	E_{ads} (eV)	E_{disp} (eV)	Angle ($^\circ$)	E_{ads} (eV)	E_{disp} (eV)	Angle ($^\circ$)	E_{ads} (eV)
C2	19.87	−1.21	−0.71	22.74	−1.31	−0.65	23.91	−1.48	−0.69	36.37	−1.64
C4	19.25	−1.33	−0.91	24.81	−1.37	−0.78	25.57	−1.58	−0.68	23.17	−1.63
C6	16.92	−1.44	−1.00	21.89	−1.49	−0.84	25.73	−1.59	−0.69	29.12	−1.73
C8	20.06	−1.63	−1.20	20.21	−1.54	−0.90	25.11	−1.62	−0.80	27.39	−1.62
C10	23.06	−1.78	−1.45	27.86	−1.62	−1.09	28.08	−1.69	−0.91	22.61	−1.66
C12	19.14	−1.88	−1.49	21.29	−1.79	−1.15	26.05	−1.75	−0.93	23.21	−1.62

from C2 to C12. At higher capping coverages (1/6 – 1/3 ML), alkylamines formed ordered overlayers on the Pt (111) surfaces with the binding energies strengthening with longer chain lengths. For C8 or longer alkyl chains, a noticeable preference to form a ($\sqrt{3} \times \sqrt{3}$) R30° (1/3 ML) alkylamine overlayer on the Pt (111) surface was observed, which is consistent with the behavior of alkane thiols on the Pd (111) surface [4]. The ordering is motivated by the rapid increase of vdW interactions among alkylamine molecules with the increasing alkylamine coating density, as suggested by Liu et al. [30]. Moreover, the tilt angle for the ($\sqrt{3} \times \sqrt{3}$) R30° pattern was much smaller than for 1/4, 1/6, 1/9 ML coverages on the Pt (111) surface, see Table 2, which could be attributed to the high alkylamine coating density. A similar phenomena was also observed in theoretical calculations of hexadecylamine adsorption on Cu surfaces [30].

We conclude that a self-assembled monolayer (SAM) of alkylamine would form on the Pt (111) surface ascribed to the increasing vdW interaction between the adsorbed alkylamines molecules and the Pt (111) surface, and alkylamine adsorption strengthens with longer chain length and higher coating density, up to 1/3 ML.

4.2. NB reduction on the alkylamine-capped Pt (111) surface

NB reduction is proposed to occur through the direct path proposed by Haber et al. on Pt surfaces, as denoted in Scheme 1 [36,37]. Intermediates including NSB and PHA are produced in the NB reduction process. Reaction free energies of reduction elementary steps were calculated on the bare Pt (111) surface and alkylamine-capped Pt (111)

surfaces. We considered NB reduction on 1/9, 1/6 and 2/9 ML alkylamine-capped Pt (111) surfaces, as we determined that NB adsorption was not favorable with higher coverages of alkylamine. As the 1/3 ML coverage was found favorable in the previous section, we conclude that saturation of the Pt (111) surface with alkylamine would block NB reduction catalysis.

4.3. NB, NSB, PHA and AN adsorption on bare and alkylamine capped Pt (111)

The NB molecule can be adsorbed either through the phenyl group (parallel configuration) or the nitro group (vertical configuration), with adsorption energies and optimized structures given in Table 3 and Fig. 2. The NB molecule preferentially adsorbs parallel to the Pt (111) surface with the phenyl group adsorbed above a fcc hollow surface site via the formation of C–Pt bonds, yielding a binding energy of −2.47 eV. Such a strong interaction between the NB molecule and the Pt (111) surface results in rehybridization of the phenyl carbons from sp^2 to sp^3 . It is not favorable for the NB molecule to adsorb vertically on the Pt (111) surface through the Pt–O bond. This is consistent with a previous theoretical study of NB adsorption on the Pt (111) surface [38] and reports that vdW interactions have a significant influence on the adsorption of phenyl groups to metal surfaces [39].

NSB, PHA, and AN molecules all preferentially adsorb with the phenyl group parallel to the bare Pt (111) surface. The binding of NSB and AN vertically adsorbed on the Pt (111) surface, however, strengthened relative to NB, since the lone pair of electrons of the N

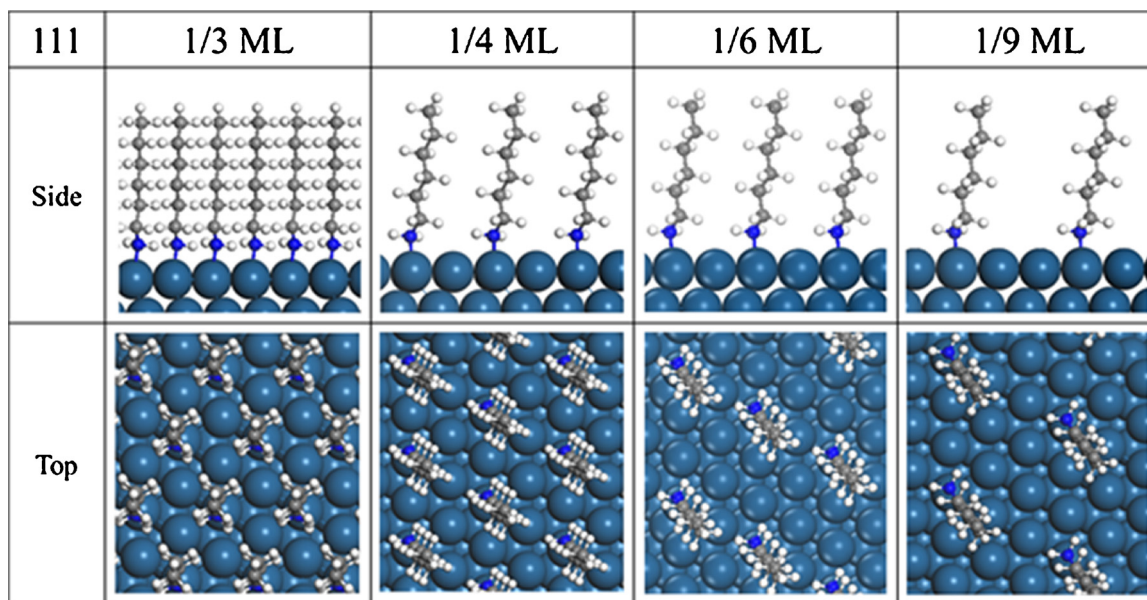
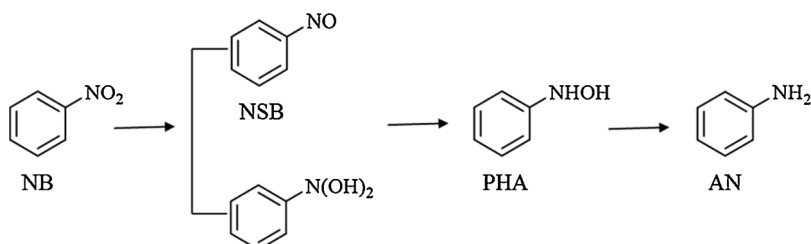


Fig. 1. Side and top views of C₆-NH₂ covered Pt (111) surfaces at different coverage (1/9, 1/6, 1/4, 1/3 ML).



Scheme 1. Direct pathway of NB reduction mechanism.

atom have a strong tendency to bind to the Pt (111) surface [38]. In general, interactions of NB, NSB, PHA and AN molecules with the Pt (111) surface mainly derive from the interaction with the phenyl group, though differences among NB, NSB, PHA and AN molecules suggest the substituent moiety impacts their binding strength, consistent with these species adsorption behavior on a Ni surface [40].

On the 1/9 ML amine-adsorbed Pt (111) surface, there is sufficient available surface for NB, NSB, PHA and AN molecules' parallel adsorption, whereas, on the crowded 1/6, 2/9 ML Pt (111) surfaces, NB, NSB, PHA and AN are forced to adsorb vertically. Adsorption configurations of NB, NSB, PHA and AN molecules on the 1/9, 1/6, and 2/9 ML alkylamine-capped Pt (111) surfaces are illustrated in Figs. 3–5, with optimized geometric properties listed in Table 4. NB, NSB, PHA and AN molecules adsorb parallel to the 1/9 ML surface, shown in Fig. 3. Their interaction with the 1/9 ML Pt (111) surface is weakened compared to the bare Pt (111) surface. The 1/9 ML amine destabilizes the planar phenyl adsorption, such that the surface-N lone pair interaction in the vertical configuration becomes competitive with the phenyl group rehybridization of NB, NSB, PHA and AN adsorbates. NB, NSB, PHA and AN adsorption in the vertical configuration, shown in Fig. 3, is strengthened on the 1/9 ML Pt (111) surface compared with the bare Pt (111) surface. This difference is due to the attractive dispersion interactions between the alkylamine and the intermediate's phenyl ring, as deduced from the dispersion energies given in Table 4. The parallel adsorption mode is preferred on the 1/9 ML Pt (111) surface for all species except PHA. But, the adsorption energy difference between the parallel (weakened) and vertical (strengthened) configurations on the 1/9 ML Pt (111) surface is reduced due to the presence of the amine.

For the 1/6 and 2/9 ML alkylamine capped Pt (111) surface, adsorption of NB, NSB, PHA and AN species in vertical adsorption mode is stronger than that on the 1/9 ML Pt (111) surface, as seen in Table 4. This is due to the more attractive dispersion interaction between adsorbed molecules and the denser coating of alkylamines, as shown in Table 4. Adsorption in the parallel mode is not possible with these denser coatings of amine. However, beyond 1/6 ML, increasing amine coverage has varying effects on the vertical adsorption binding strength. For example, the adsorption energy of NSB via N and O atoms on the 2/9 ML Pt (111) surface was 0.02 eV weaker than that on the 1/6 ML Pt (111) surface. Vertical adsorption configurations of NB, NSB, PHA and AN on the 1/6 and 2/9 ML Pt (111) surfaces are illustrated in

Figs. 4 and 5.

4.4. Elementary step thermodynamics of NB reduction on alkylamine capped Pt (111) surfaces

Reaction free energy changes for the elementary steps in NB reduction to AN on the bare Pt (111) surface in both parallel and vertical adsorption modes are summarized in Table 5. NB reduction can go through either a C₆H₅NO or a C₆H₅NO₂H₂ intermediate in the second step, as depicted in Scheme 1. C₆H₅NO formation from C₆H₅NO₂H in the second step is more favorable than C₆H₅NO₂H₂ formation, in either a parallel or vertical adsorption mode, as given in Table 5. This is consistent with the detection of NSB as an intermediate in NB reduction on a Pt catalyst.[41] The NB* reduction energetics do not show any significant qualitative differences whether the intermediates are in the parallel or vertical adsorption, though preferential flat adsorption suggests this mode should be considered for the bare Pt (111) surface. Reaction free energies of all the elementary steps in NB reduction process were negative with molecules in parallel adsorption configurations (Table 5), which was also observed on the Ni (111) surface. [40]

Reaction free energies of NB reduction on an alkylamine-capped Pt (111) surface are summarized in Table 5 and Fig. 6. NB reduction to AN was also more likely to go through C₆H₅NO rather than C₆H₅NO₂H₂ in the second step on the alkylamine-capped Pt (111) surfaces (1/9, 1/6, 2/9 ML), as C₆H₅NO₂H₂ formation is thermodynamically unfavorable (Table 5). NB reduction free energy diagrams in both parallel and vertical adsorption mode on the 1/9 ML surface are plotted in Fig. S2. NB reduction did not show clear difference either in parallel or vertical adsorption mode on 1/9 ML Pt (111) surface in terms of elementary step thermodynamics. All elementary steps for NB* reduction to AN in the vertical adsorption mode are downhill.

On the 1/6 ML and 2/9 ML alkylamine capped Pt (111) surfaces, NB, AN as well as all intermediates are forced to adsorb vertically. Every elementary step of NB* reduction to AN on the 1/6 ML alkylamine-capped Pt (111) surface is exergonic, indicating NB reduction on the 1/6 ML Pt (111) surface is thermodynamically favorable (Table 5). The reaction free energy of C₆H₅NOH* formation from NSB was positive on the 2/9 ML Pt (111) surface, indicating this step was thermodynamically unfavorable (Table 5). The interaction of C₆H₅NOH* with the 2/9 ML Pt (111) surface via the N atom was weakened at this higher

Table 3
NB, NSB, PHA and AN adsorption energy on the bare (3 × 3) Pt (111) surface. Unit: eV.

	NB		NSB		PHA		AN	
	E _{ads} (eV)	E _{disp} (eV)						
flat	t	-2.07	-1.54	t	-2.07	-1.55	t	-2.24
	fcc	-2.47		fcc	-2.47		fcc	-2.49
	hcp	-2.45		hcp	-2.45		hcp	-2.24
upright	t-O	-0.60	-0.69	t-O	-0.90	-0.80	t1	-0.82
	t-O-O	-0.59		t-N-O	-1.78		t2	-0.83
	b-O-O	-0.63		b-N-O	-1.80		b	-0.92
							-0.67	-0.67
							b	-0.37

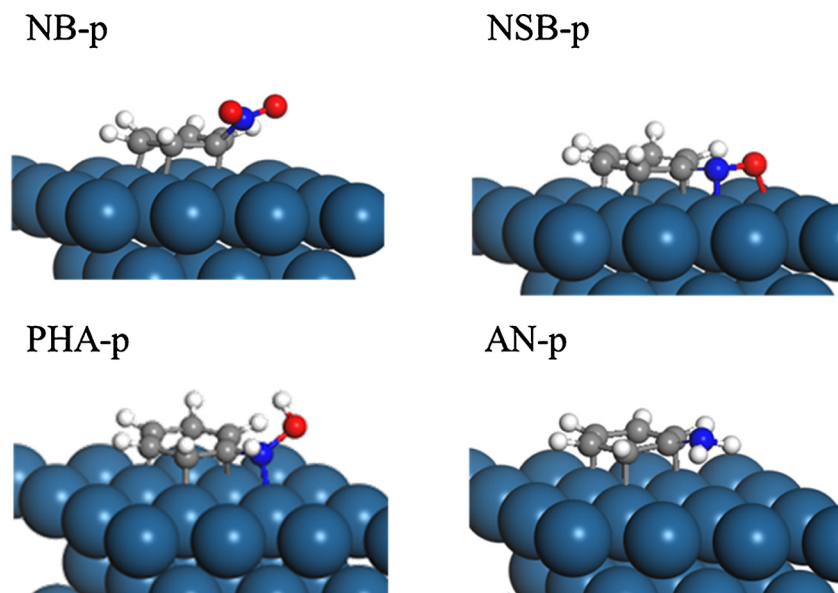


Fig. 2. DFT calculated structures for the most stable molecules parallel (p) adsorption structures for NB, NSB, PHA and AN on the bare (3×3) Pt (111) catalyst surface. (Pt/blue, carbon/grey, hydrogen/white, oxygen/red, nitrogen/blue) (For interpretation of the references to colour in this figure legend, the reader is referred to the web version of this article).

coating density, compared with the NSB^* interaction through N and O atoms. Other than this step, all the elementary steps in NB^* reduction on the 2/9 ML Pt (111) surface were thermodynamically favorable (Table 5).

We conclude that alkylamine packing densities up to 2/9 ML still leave enough open surface for hydrogenation to proceed, while forcing all species to interact through the N-group rather than through parallel adsorption of the phenyl ring. Interactions between the various NB-derived intermediates and the amines vary, causing differences in elementary reaction at different coverages. Collectively, these interactions do not prevent hydrogenation at low amine coverage. All adsorbates are weakened by amine co-adsorption, which may help increase the

reduction rate by preventing strong binding of the phenyl group that could block the surface during reduction on the non-modified surface. However, the amine will block part of the surface which could decrease the overall activity. With these competing influences, the predicted impact of amine co-adsorption on the overall hydrogenation rate is difficult to discern without microkinetic modeling.

Strong binding of NB or the other intermediates have the potential to displace amines from the surface. We do not directly observe this phenomena during optimization of adsorbates within the 1/9, 1/6, 2/9 ML amines on the Pt (111) surface, as shown in Figs. 3–5. As reported in Table 2, the binding energies of the short chain amines (C2–C6) weaken with increasing coverage, making high coverage adsorption of

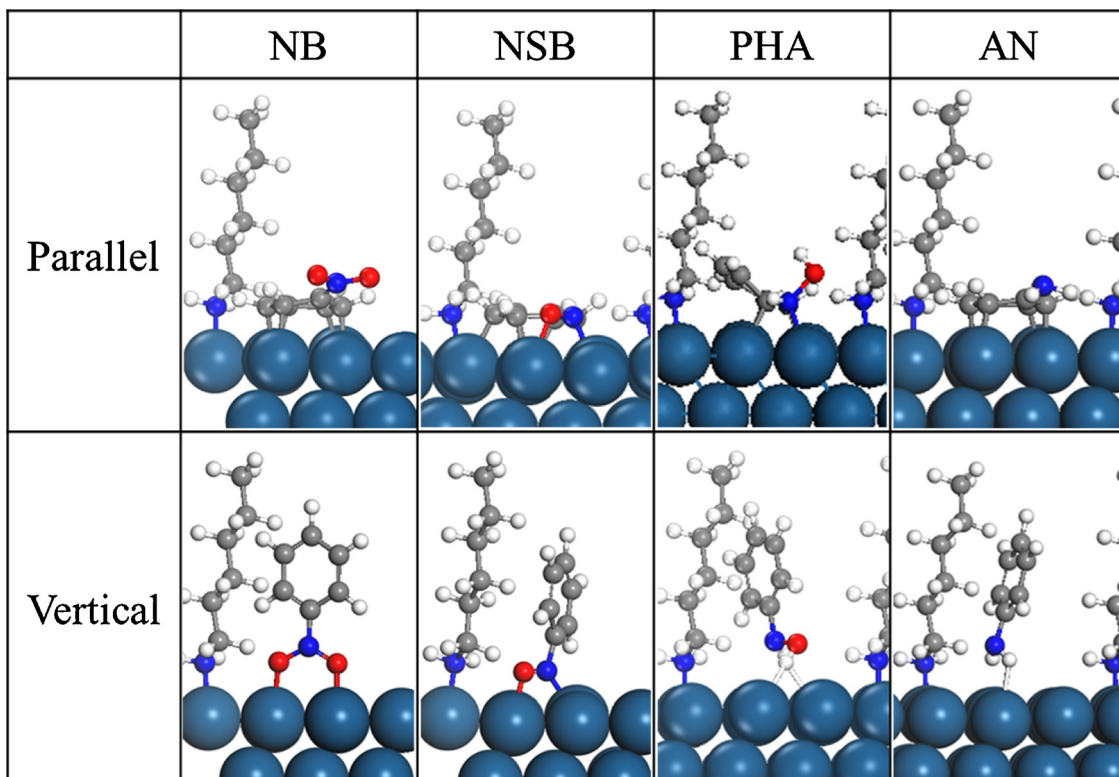


Fig. 3. The most stable parallel and vertical adsorption configurations for NB, NSB, PHA and AN on the 1/9 ML alkylamine capped Pt (111) catalyst surface.

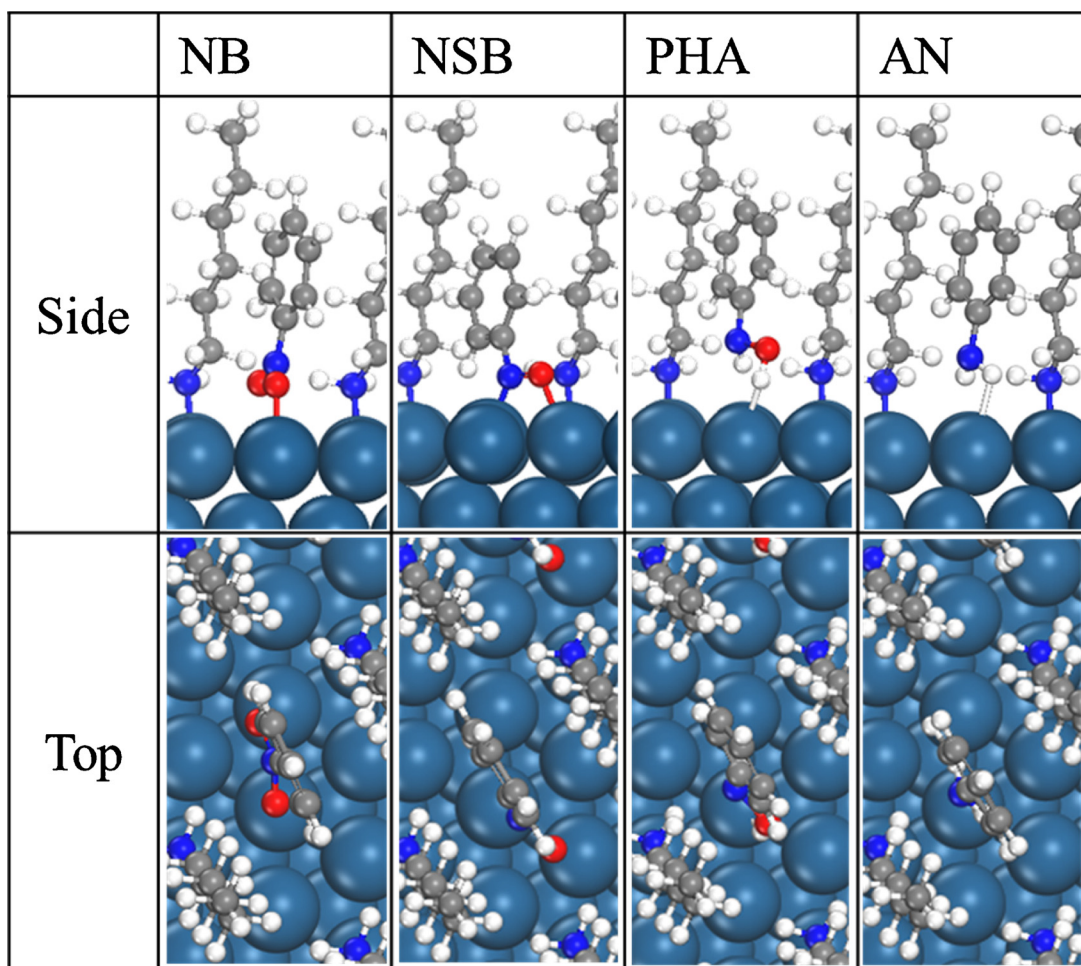


Fig. 4. Side and top views of the most stable vertical adsorption configurations for NB, NSB, PHA and AN on the 1/6 ML alkylamine capped Pt (111) surface.

short chain amines weaker than adsorption of NB and some intermediates. This suggests that adsorbates may promote some extent of amine desorption, helping to tailor the surface towards an intermediate coverage that still allows for NB reduction. Makosch et al. observed changes in the impact of organic modifiers with time that they attributed to displacement of modifiers by reactants and intermediates [42]. Ramirez et al. reported that the mobility of Pt-adsorbed amines increased with H₂ addition [34].

4.5. NB selective reduction to PHA

As we have determined that hydrogenation may proceed in the presence of low-coverage (~1/6 ML) amine, we now consider how the amine affects the selectivity to PHA versus AN. To examine this selectivity, we compute the activation barriers for PHA hydrogenation to C₆H₅NH on the bare and alkylamine capped Pt (111) surfaces. Desorption of PHA would give the desired fluid phase product, whereas further hydrogenation leads to the non-selective hydrogenation to AN. The hydrogenation transition states are shown in Fig. 7. Calculated energy barriers are also compared with the PHA desorption energy to explore the selectivity of NB reduction on the bare and alkylamine capped Pt (111) surfaces (1/9 ML, 1/6 ML and 2/9 ML) in Table 6.

On the bare Pt (111) surface with PHA in the parallel adsorption mode, the energy barrier for C₆H₅NH formation is 0.65 eV (Fig. 7, Table 6). The PHA N–O bond is broken in the transition state (Fig. 7, Pt (111) TS1), consistent with Sheng's research [38]. The desorption energy of PHA from the bare Pt (111) surface was 2.49 eV (Table 3), about 4 times the hydrogenation energy barrier. The DFT desorption energy is

used to approximate the activation barrier to unimolecular adsorption, prior to obtaining the entropic freedom that would contribute to the fluid phase chemical potential. This hydrogenation of PHA will greatly outpace desorption, such that PHA tends to reduce to C₆H₅NH on the bare Pt (111) surface. For the 1/9 ML amine-modified Pt (111) surface, both parallel and vertical adsorption modes were taken into consideration. For the parallel adsorption mode, the transition state of PHA reduction to C₆H₅NH was similar in structure to that on the bare surface, with an energy barrier of 0.32 eV (Fig. 7, 1/9 ML/flat, TS1), lower than that on the bare Pt (111) surface. This indicates that low-coverage of alkyl amine could favor PHA hydrogenation in parallel adsorption mode. The desorption energy of PHA from the 1/9 ML Pt (111) surface is 0.94 eV (Table 4), about two fold higher than the energy barrier of PHA reduction.

Vertical adsorption of PHA on alkyl amine capped Pt (111) surfaces leads to a significant increase in the hydrogenation barrier. On the 1/9 ML Pt (111) surface, the transition state of PHA* hydrogenation in vertical adsorption mode again shows the N–O bond broken. The hydrogenation barrier is 1.02 eV on the 1/9 ML amine Pt (111) surface, much higher than that in parallel adsorption mode. Increasing the amine coverage above 1/9 ML further increased the PHA* hydrogenation barriers to 1.29 (1/6 ML) and 1.81 eV (2/9 ML), indicating increased alkyl amine on the Pt (111) surfaces make PHA hydrogenation, including breaking of the N–O bond, more difficult. In forcing PHA adsorption in the vertical mode, these intermediate amine coverages lead to slower hydrogenation, with barriers similar to the PHA desorption energies. However, it should be noted that using the desorption energies in Tables 4 and 6 as a direct measure of the desorption barrier

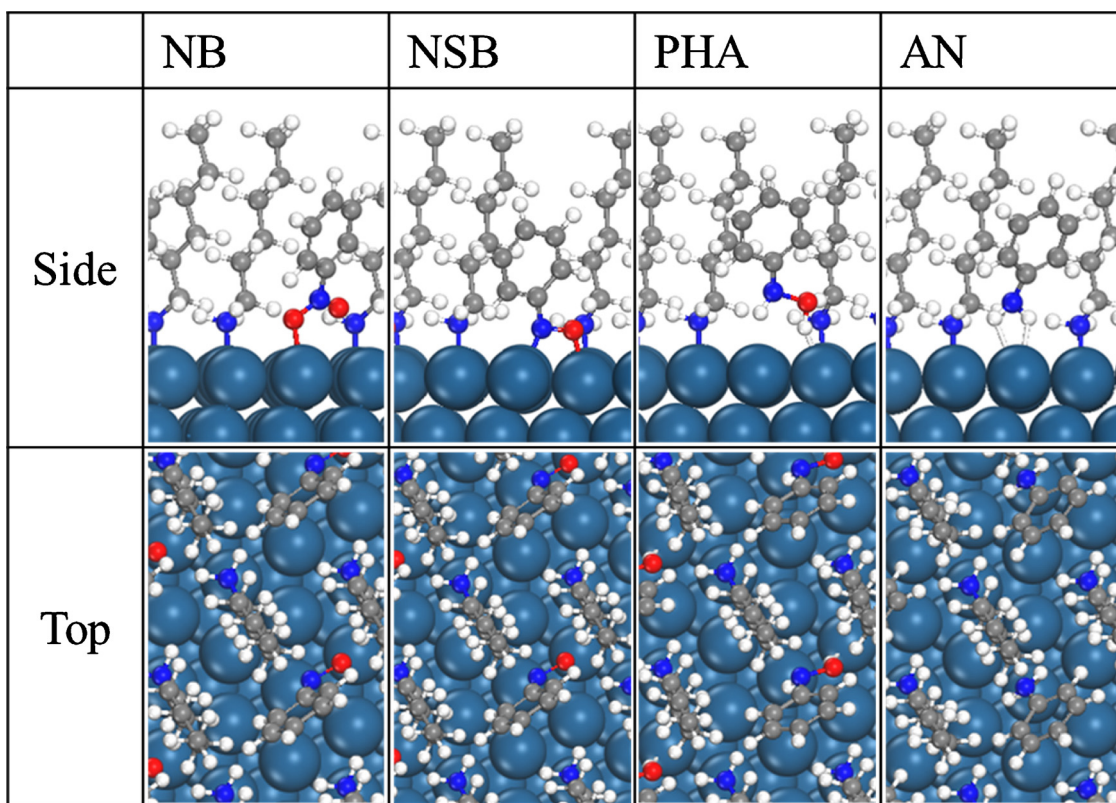


Fig. 5. Side and top views of the most stable vertical adsorption configurations for NB, NSB, PHA and AN adsorbed vertically onto the 2/9 ML alkylamine capped Pt (111) surface.

Table 4

NB, NSB, PHA and AN adsorption energies and dispersion energies on alkylamine capped Pt (111) surfaces (1/9, 1/6 and 2/9 ML).

	NB		NSB		PHA		AN	
	E_{ads} (eV)	ΔE_{disp} (eV)						
1/9 ML flat	-1.59	-1.85	-2.41	-1.81	-0.94	-1.93	-1.58	-1.77
1/9 ML upright	-0.77	-0.98	-1.89	-1.05	-1.35	-0.97	-1.09	-0.86
1/6 ML upright	-0.92	-1.38	-2.29	-1.46	-1.59	-1.31	-1.31	-1.23
2/9 ML upright	-1.31	-1.31	-2.27	-1.42	-1.76	-1.22	-1.31	-1.20

Table 5

Calculated reaction energies (ΔG) for all elementary steps in NB reduction to AN on the 1/9 ML, 1/6, and 2/9 alkylamine capped Pt (111) surface. Unit: eV.

Steps	ΔG					
	Pt (111) Flat	Pt (111) Upright	1/9 ML Flat	1/9 ML Upright	1/6 ML	2/9 ML
$NB^* + 1/2H_2 \rightarrow C_6H_5NO_2H^*$	-0.03	-0.10	-0.85	-0.62	-0.53	-0.04
$C_6H_5NO_2H^* + 1/2H_2 \rightarrow NSB^* + H_2O$	-1.76	-2.05	-0.88	-1.90	-1.72	-1.97
$C_6H_5NO_2H^* + 1/2H_2 \rightarrow C_6H_5NO_2H_2^*$	0.46	-0.27	2.66	2.30	2.16	
$NSB^* + 1/2H_2 \rightarrow C_6H_5NOH^*$	0.06	0.03	-0.50	0.22	-0.14	0.37
$C_6H_5NO_2H_2^* + 1/2H_2 \rightarrow C_6H_5NOH^* + H_2O$	-2.16	-1.75	-3.16	-2.08	-2.30	
$C_6H_5NOH^* + 1/2H_2 \rightarrow PHA^*$	-0.14	-0.03	0.07	-0.34	-0.38	-1.15
$PHA^* + 1/2H_2 \rightarrow PHA^* + H^*$	-0.42	-0.24	-0.50	-0.42	-0.41	-0.44
$PHA^* + H^* \rightarrow C_6H_5NH^* + H_2O$	1.56	-0.21	-2.72	-1.39	-1.59	-0.95
$C_6H_5NH^* + 1/2H_2 \rightarrow AN^*$	-0.25	-0.62	-0.56	-0.55	-0.69	-0.72

overestimates the desorption barrier. The desorption energies represent the energy needed to move the PHA from the surface to the vacuum, as an isolated molecule. However, the actual desorbed state would continue to have vdW interactions either higher in an amine layer or in solution, such that the effective barrier to desorption would be lower.

In summary, vertical adsorption of PHA, induced by amine

modification of the Pt (111) surface, raises the barrier to PHA hydrogenation and reduces the PHA desorption energy, promoting selective reduction to PHA over AN. The major impact of surface modification is a steric effect that inhibits the parallel adsorption of the phenyl ring, and thus inhibits NB molecule over-hydrogenation to AN. The impact of steric effects in directing partial-hydrogenation selectivity was similarly

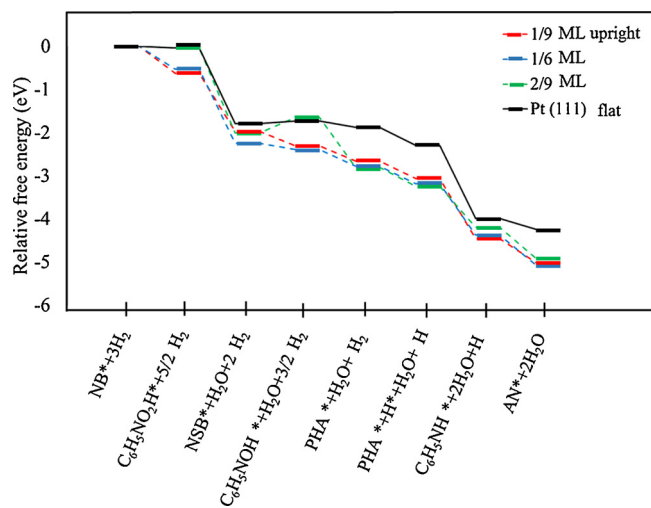


Fig. 6. Energy diagrams of NB reduction to AN on the bare (3×3) Pt (111) surface and the 1/9, 1/6, 2/9 ML alkylamine capped Pt (111) surfaces.

observed for α, β -unsaturated aldehydes selective reduction catalyzed by amine-capped platinum-cobalt nanocrystals [6]. Varying the amine coverage might be used to tune the selectivity, with very low coverages still allowing for AN formation, intermediate coverages for PHA formation, and high packing densities blocking all reactant access to the surface. Regrettably, we cannot directly comment on the coverage of amine present in experimental studies of amine modification. For short chain amines, we do observe that adsorption becomes weaker with increasing coverage, suggesting it is plausible that an intermediate coverage is obtained that allows for NB reduction to occur.

As the role of the amine is to block parallel adsorption of the phenyl

ring, we examined whether the substitution of “inert” metal atoms into the Pt surface could promote a similar effect on selective hydrogenation. NB reduction to PHA on Pt_2Sn , Pt_2Zn and PtZn_2 surfaces was examined, as addition of Zn metal has been reported to promote selective NB reduction to PHA [43–46]. Parallel and vertical adsorption modes of NB are illustrated in Fig. S3 with the adsorption energies given in Table S1. NB prefers adsorption in the parallel configuration on Pt_2Sn (111), Pt_2Zn (111), and PtZn_2 (111) surfaces. On the PtSn_2 surface, NB adsorbs only through weak physisorption, showing no rehybridization of the C atoms [43,45]. On the Pt_2Zn and PtZn_2 surfaces, NB chemisorbs through C–Zn, C–Pt or O–Pt and O–Zn bonds as illustrated in Fig. S3.

Energy barriers, reaction energies and desorption energies of PHA hydrogenation on the bimetallic surfaces are given in Table 6. In general, PHA hydrogenation either in parallel or vertical adsorption mode all show slightly higher energy barriers for PHA^* hydrogenation than on the bare Pt (111) surface. The increases in hydrogenation barrier are not as significant as those observed with amine co-adsorption. An exception is the PtZn_2 surface with flat binding, where the barrier to PHA hydrogenation is significantly increased. This is a symptom of the specific ring orientation used to remain consistent with other surfaces, and re-orientation to the vertical mode on this surface would still allow for hydrogenation over a relatively low barrier. Pt_2Sn , Pt_2Zn and PtZn_2 do not successfully motivate vertical adsorption of PHA, and the increases in PHA hydrogenation barrier are not as significant as for amine co-adsorption. We conclude that amine surface crowding is more successful in inducing vertical adsorption configurations that allow for hydrogenation to PHA, and preferential desorption of PHA over further hydrogenation.

5. Conclusions

We have shown that alkylamine-modified Pt (111) catalysts show

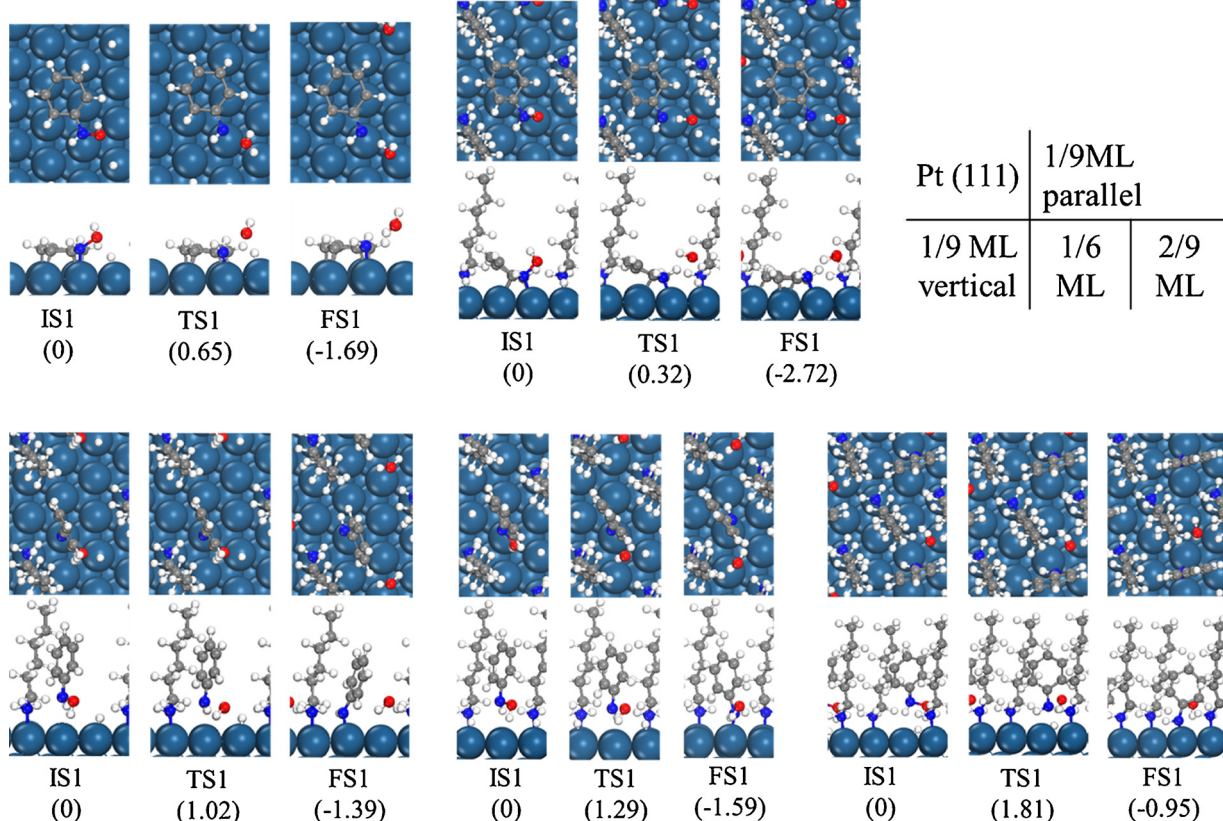


Fig. 7. Top (above) and side (below) views of all the optimized geometries for PHA reduction to $\text{C}_6\text{H}_5\text{NH}$ on the bare Pt (111) surface and the 1/9, 1/6 as well as 2/9 ML alkylamine capped Pt (111) surfaces.

Table 6

Calculated PHA desorption energy, hydrogenation energy barrier (E_a), and hydrogenation reaction energy (ΔG) for PHA reduction to C_6H_5NH on Pt (111), amine-modified Pt (111), and Pt-Sn/Zn bimetallic surfaces. Unit: eV.

	amine-capped Pt (111) surface					Pt ₂ Sn	Pt ₂ Zn	PtZn ₂	Pt ₂ Zn	PtZn ₂
	no amine	1/9 ML/ Flat	1/9 ML/ Upright	1/6 ML	2/9 ML	Flat	Flat	Flat	Upright	Upright
PHA desorption energy	2.49	1.70	1.35	1.59	1.76	1.21	2.03	1.50	1.48	1.41
E_a	0.65	0.32	1.02	1.29	1.81	0.63	0.98	1.58	0.68	0.77
C_6H_5NH formation energy (ΔG)	-1.69	-2.72	-2.23	-1.59	-0.95	-1.56	-2.80	-2.86	-2.23	-2.01

selectivity in the NB reduction process by reorienting adsorbed intermediates such that hydrogenation to PHA is favorable, but PHA binding is weakened to avoid over-hydrogenation. By using the proper intermediate coverage of alkylamines on Pt (111) surfaces, NB can be selectively reduced to PHA. The non-modified surface preferentially reduces NB to AN, as adsorption through the phenyl moiety prevents PHA desorption and facilitates further hydrogenation. Modifying metal catalysts with alkylamines provides a means to control active-site availability and alter the steric interactions of reactants and intermediates in the third dimension above the surface. Thus, surface modification of metal catalysts can serve as an effective strategy (or complement) to control selectivity.

Acknowledgements

L. Gong acknowledges scholarship from the China Scholarship Council for a joint PhD student. Yang Mu wishes to thank the Natural Science Foundation of China (51538012) for financially supporting this study. This work used the Extreme Science and Engineering Discovery Environment (XSEDE), which is supported by National Science Foundation grant number ACI-1053575.

Appendix A. Supplementary data

Supplementary material related to this article can be found, in the online version, at doi:<https://doi.org/10.1016/j.apcatb.2018.05.015>.

References

- [1] K. Miyabayashi, H. Nishihara, M. Miyake, Langmuir 30 (2014) 2936–2942.
- [2] S.G. Kwon, G. Krylova, A. Sumer, M.M. Schwartz, E.E. Bunel, C.L. Marshall, S. Chattopadhyay, B. Lee, J. Jellinek, E.V. Shevchenko, Nano. Lett. 12 (2012) 5382–5388.
- [3] R.A. Masitas, I.V. Khachian, B.L. Bill, F.P. Zamborini, Langmuir 30 (2014) 13075–13084.
- [4] G. Kumar, C.H. Lien, M.J. Janik, J.W. Medlin, Acs Catal. 6 (2016) 5086–5094.
- [5] S.H. Pang, C.A. Schoenbaum, D.K. Schwartz, J.W. Medlin, Nat. Commun. 4 (2013).
- [6] B.H. Wu, H.Q. Huang, J. Yang, N.F. Zheng, G. Fu, Angew. Chem. Int. Ed. 51 (2012) 3440–3443.
- [7] G.X. Chen, C.F. Xu, X.Q. Huang, J.Y. Ye, L. Gu, G. Li, Z.C. Tang, B.H. Wu, H.Y. Yang, Z.P. Zhao, Z.Y. Zhou, G. Fu, N.F. Zheng, Nat. Mater. 15 (2016) 564–569.
- [8] M.A. Rodrigo, N. Oturan, M.A. Oturan, Chem. Rev. 114 (2014) 8720–8745.
- [9] C. Liu, A.Y. Zhang, D.N. Pei, H.Q. Yu, Environ. Sci. Technol. 50 (2016) 5234–5242.
- [10] Q. Xiao, S. Sarina, E.R. Waclawik, J.F. Jia, J. Chang, J.D. Riches, H.S. Wu, Z.F. Zheng, H.Y. Zhu, Acs. Catal. 6 (2016) 1744–1753.
- [11] X.H. Lu, J. He, R. Jing, P.P. Tao, R.F. Nie, D. Zhou, Q.H. Xia, Sci. Rep.-Uk. 7 (2017).
- [12] X.N. Guo, C.H. Hao, G.Q. Jin, H.Y. Zhu, X.Y. Guo, Angew. Chem. Int. Ed. 53 (2014) 1973–1977.
- [13] S.L. Karwa, R.A. Rajadhyaksha, Ind. Eng. Chem. Res. 26 (1987) 1746–1750.
- [14] D.Q. Niu, K. Zhao, J. Am. Chem. Soc. 121 (1999) 2456–2459.
- [15] C.K. Svensson, Chem. Res. Toxicol. 16 (2003) 1035–1043.
- [16] F. Ahmad, J.B. Hughes, Environ. Sci. Technol. 36 (2002) 4370–4381.
- [17] R.S. Srivastava, K.M. Nicholas, J. Am. Chem. Soc. 119 (1997) 3302–3310.
- [18] L.X. Li, T.V. Marolla, L.J. Nadeau, J.C. Spain, Ind. Eng. Chem. Res. 46 (2007) 6840–6846.
- [19] A.D. Shebalova, V.N. Kravtsova, T.A. Bolshinskova, E.V. Selyaeva, M.L. Khidekel, Br. Acad. Sci. USSR. 24 (1975) 1556–1557.
- [20] E.H. Boymans, P.T. Witte, D. Vogt, Catal. Sci. Technol. 5 (2015) 176–183.
- [21] L.A. Carpiño, C.A. Giza, B.A. Carpiño, J. Am. Chem. Soc. 81 (1959) 955–957.
- [22] Q.X. Shi, R.W. Lu, K. Jin, Z.X. Zhang, D. Zhao, Chem. Lett. 35 (2006) 226–227.
- [23] S. Ung, A. Falguieres, A. Guy, C. Ferroud, Tetrahedron Lett. 46 (2005) 5913–5917.
- [24] H. Feuer, B.F. Vincent, J. Am. Chem. Soc. 84 (1962) 3771–3772.
- [25] F.M. Cordero, I. Barile, F. De Sarlo, A. Brandi, Tetrahedron Lett. 40 (1999) 6657–6660.
- [26] F. Li, J.N. Cui, X.H. Qian, Z.A. Rong, Y. Xiao, Chem. Commun. (2005) 1901–1903.
- [27] Y. Takenaka, T. Kiyosu, J.C. Choi, T. Sakakura, H. Yasuda, Green Chem. 11 (2009) 1385–1390.
- [28] G. Kresse, J. Furthmüller, Phys. Rev. B. 54 (1996) 11169–11186.
- [29] G. Kresse, J. Furthmüller, Comp. Mater. Sci. 6 (1996) 15–50.
- [30] Z. Liu, Y.M. Huang, Q. Xiao, H.Y. Zhu, Green Chem. 18 (2016) 817–825.
- [31] G. Henkelman, B.P. Uberuaga, H. Jonsson, J. Chem. Phys. 113 (2000) 9901–9904.
- [32] H.J. Monkhorst, J.D. Pack, Phys. Rev. B. 13 (1976) 5188–5192.
- [33] I.T. McCrum, M.A. Hickner, M.J. Janik, Langmuir 33 (2017) 7043–7052.
- [34] E. Ramirez, L. Erades, K. Philippot, P. Lecante, B. Chaudret, Adv. Funct. Mater. 17 (2007) 2219–2228.
- [35] R.C. Hoft, M.J. Ford, A.M. McDonagh, M.B. Cortie, J. Phys. Chem. C 111 (2007) 1386–13891.
- [36] S. Galvagno, A. Donato, G. Neri, R. Pietropaolo, Z. Poltarzewski, J. Mol. Catal. 42 (1987) 379–387.
- [37] L.Y. Zhang, J.H. Jiang, W. Shi, S.J. Xia, Z.M. Ni, X.C. Xiao, Rsc. Adv. 5 (2015) 34319–34326.
- [38] T. Sheng, Y.J. Qi, X. Lin, P. Hu, S.G. Sun, W.F. Lin, Chem. Eng. J. 293 (2016) 337–344.
- [39] W. Liu, J. Carrasco, B. Santra, A. Michaelides, M. Scheffler, A. Tkatchenko, Phys. Rev. B. 86 (2012).
- [40] A. Mahata, R.K. Rai, I. Choudhuri, S.K. Singh, B. Pathak, Phys. Chem. Chem. Phys. 16 (2014) 26365–26374.
- [41] R.F. Nie, J.H. Wang, L.N. Wang, Y. Qin, P. Chen, Z.Y. Hou, Carbon 50 (2012) 586–596.
- [42] M. Makosch, W.I. Lin, V. Bumbalek, J. Sa, J.W. Medlin, K. Hungerbuhler, J.A. van Bokhoven, Acs. Catal. 2 (2012) 2079–2081.
- [43] L. Nykanen, K. Honkala, J. Phys. Chem. C. 115 (2011) 9578–9586.
- [44] W.T. Yu, M.D. Porosoff, J.G.G. Chen, Chem. Rev. 112 (2012) 5780–5817.
- [45] J. Breitbach, D. Franke, G. Hamm, C. Becker, K. Wandelt, Surf. Sci. 507 (2002) 18–22.
- [46] S.J. Liu, Y.H. Wang, J.Y. Jiang, Z.L. Jin, Green Chem. 11 (2009) 1397–1400.